Development 128, 2175-2186 (2001)
Printed in Great Britain © The Company of Biologists Limited 2001
DEV2708

sprouty4 acts in vivo as a feedback-induced antagonist of FGF signaling in zebrafish

Maximilian Fürthauer[1], Frank Reifers[2], Michael Brand[2], Bernard Thisse[1] and Christine Thisse[1,*]

[1]Institut de Génétique et Biologie Moléculaire et Cellulaire, CNRS/INSERM/ULP, BP 163, 67404 Illkirch cedex, CU de Strasbourg, France
[2]Max Planck Institute for Cell Biology and Genetics, Dresden. c/o Department of Neurobiology University of Heidelberg Im Neuenheimer Feld 364 D-69120 Heidelberg, Germany
*Author for correspondence (e-mail: thisse@igbmc.u-strasbg.fr)

Accepted 26 March 2001

SUMMARY

In looking for novel factors involved in the regulation of the fibroblast growth factor (FGF) signaling pathway, we have isolated a zebrafish *sprouty4* gene, based on its extensive similarities with the expression patterns of both *fgf8* and *fgf3*. Through gain- and loss-of-function experiments, we demonstrate that Fgf8 and Fgf3 act in vivo to induce the expression of Spry4, which in turn can inhibit activity of these growth factors. When overexpressed at low doses, Spry4 induces loss of cerebellum and reduction in size of the otic vesicle, thereby mimicking the *fgf8/acerebellar* mutant phenotype. Injections of high doses of Spry4 cause ventralization of the embryo, an opposite phenotype to the dorsalisation induced by overexpression of Fgf8 or Fgf3. Conversely we have shown that inhibition of Spry4 function through injection of antisense morpholino oligonucleotide leads to a weak dorsalization of the embryo, the phenotype expected for an upregulation of Fgf8 or Fgf3 signaling pathway. Finally, we show that Spry4 interferes with FGF signaling downstream of the FGF receptor 1 (FGFR1). In addition, our analysis reveals that signaling through FGFR1/Ras/mitogen-activated protein kinase pathway is involved, not in mesoderm induction, but in the control of the dorsoventral patterning via the regulation of bone morphogenetic protein (BMP) expression.

Key words: BMP, Sprouty4, FGF3, FGF8, FGFR, ERK, MAPK, Ras, Morpholino, Zebrafish

INTRODUCTION

Throughout embryonic and adult life, members of the fibroblast growth factor (FGF) family of secreted signaling molecules are implicated in the regulation of cell survival, proliferation, migration and differentiation (Fernig and Gallagher, 1994). At early stages of vertebrate embryogenesis FGFs have been shown to be implicated in the induction of the mesoderm (Amaya et al., 1991; Yamaguchi et al., 1994), as well as the establishment of the anteroposterior and dorsoventral body axes (Fürthauer et al., 1997; Lamb and Harland, 1995; Partanen et al., 1998). At later stages, FGF signaling is required for various aspects of organogenesis, including the growth and patterning of the brain (Reifers et al., 1998), the initiation and outgrowth of the limb buds (Martin, 1999) and tooth morphogenesis (Thesleff and Sharpe, 1997). Some of the functions of FGFs have been conserved throughout evolution: both in *Drosophila* and mouse embryos the outgrowth and branching of the respiratory system is dependent on the activity of this signaling pathway (Metzger and Krasnow, 1999).

Studies in vertebrates have revealed the existence of at least 20 different FGFs that are characterized by the presence of a conserved 120 amino acid core region. FGFs elicit their cellular response through the binding to transmembrane tyrosine kinase FGF receptors (FGFRs). The four existing FGFR genes encode seven receptor isoforms with different binding affinities for the various FGFs (Ornitz et al., 1996). Moreover binding of FGFs to heparan sulfate proteoglycans is crucial for efficient receptor stimulation (Lin et al., 1999). FGF binding induces the dimerisation of FGFRs, therefore allowing the transphosphorylation of several cytoplasmic tyrosine residues. This modification leads to the recruitment and phosphorylation of the lipid-anchored protein FRS2, which then interacts with the SH2 domain-containing adaptor protein Grb2 (Kouhara et al., 1997). Grb2 then allows the binding of the guanine nucleotide exchange factor Sos, which mediates the activation of the membrane-bound monomeric G-protein Ras (Lowenstein et al., 1992). This in turn induces the activation of a kinase cascade comprising Raf, mitogen-activated protein kinase (MAPK) and MAPK kinase (MEK), the last member of which finally enters the nucleus and phosphorylates target transcription factors (Sternberg and Alberola-Ila, 1998).

Recent genetic studies in *Drosophila* have led to the isolation of the novel gene *sprouty* (*spry*) which antagonizes FGF signaling during tracheal morphogenesis (Hacohen et al., 1998). Subsequent work has revealed that Spry not only

interferes with signaling by FGFRs, but also with signaling by the epidermal growth factor (EGF) receptor, torso and sevenless receptor tyrosine kinases (RTK) (Casci et al., 1999; Kramer et al., 1999; Reich et al., 1999). Spry has been suggested to act as general antagonist of RTK-induced Ras signaling through the interaction with the docking protein Drk (the *Drosophila* Grb2 homolog) and the GTPase Gap1, which acts as an inhibitor of Ras activation (Casci et al., 1999).

Studies in vertebrates have revealed the existence of several *spry* homologs in mouse and chicken. These genes are expressed in regions of ongoing FGF signaling and can be induced locally through the implantation of beads soaked in recombinant FGF proteins (Chambers et al., 2000; Minowada et al., 1999). Moreover, studies of mouse lung development suggest that, as in *Drosophila*, Spry acts as an inhibitor of branching morphogenesis (Tefft et al., 1999).

In the course of a large-scale in situ hybridization screen of embryonic gene expressions, we have identified a zebrafish *sprouty4* homolog, owing to its coexpression with *fgf8* and *fgf3*. We show that Fgf8 and Fgf3 act in vivo to induce the expression of Spry4, which antagonizes their activity by acting downstream of FGFR1.

MATERIALS AND METHODS

Whole-mount in situ hybridization

For *spry4*, a 720 bp *Bam*HI/*Xho*I 3′UTR fragment was subcloned in the corresponding sites of pBSKII(+). For *fgf3* (Kiefer et al., 1996), a 560 bp 3′UTR fragment was amplified by RT-PCR using the primers GGATCCCTCTCTCTTGACACAGATGG and CTCGAGTTGAG-ATTGGAAGGGTAG, and subcloned in the *Bam*HI/*Xho*I sites of pBSKII(+). For probe synthesis, plasmids were linearized with *Bam*HI and RNA transcribed with T7 RNA polymerase. In situ hybridization was performed as described (Thisse and Thisse, http://www-igbmc.u-strasbg.fr/zf_info/zbook/chapt9/9.82.html).
CG1061 as well as CB588 were isolated within the course of our large-scale in situ hybridization screen (B.T. and C. T., unpublished).

Plasmids

Fragments of zebrafish cDNA coding for FGFR1, FGFR2, FGFR3 and used as probe for in situ were as described (Poss et al., 2000). Constructs encoding constitutively activated FGFR1 and FGFR4 have already been described (Umbhauer et al., 2000).

Whole-mount MAPK immunostaining

Embryos were fixed for 24 hours in 4% PFA at 4°C, dehydrated by 10 minute incubations in 25, 50, 75 and 100% ethanol and stored in 100% ethanol at –20°C. For antibody staining, embryos were rehydrated by 10 minute incubations in 75, 50 and 25% ethanol, washed five times for 5 minutes in PBT (phosphate-buffered saline (PBS) 1×, 0,1% Tween 20) and preadsorbed for several hours at room temperature by incubation in PBTSB (PBT, 10% sheep serum, 10 mg/ml bovine serum albumin). Embryos were then incubated overnight at 4°C with a 1:10,000 dilution in PBTSB of an anti-activated-MAPK antibody coupled to alkaline phosphatase (Sigma, A3713). Unbound antibody was washed off with eight 15 minute washes in PBT. For the staining reaction, embryos were processed as for whole-mount in situ hybridization.

mRNA and morpholino injections

The *spry4* open reading frame (ORF) was PCR amplified using the primers ATCGATTGAGGAACACGACCTACA and CTCGAGGAA-GGTCCTGCAAACCAT, and subcloned into the *Cla*I/*Xho*I sites of pCS2+. For *fgf3* (Kiefer et al., 1996), the ORF was amplified by RT-PCR using the primers GAATTCATTCCAGCGAGATTTTGCCG and TCTAGACCATCTGTGTCAAGAGAGAG, and subcloned into the *Eco*RI/*Xba*I sites of pCS2+. For microinjection plasmids were linearized with *Not*I and sense RNA transcribed with SP6 RNA polymerase using the mMessage mMachine Kit (Ambion).

Morpholinos (Gene Tools) were resuspended in sterile water, stored at –20°C as a 4 mM stock solution and diluted before use to the appropriate concentration. The sequences of the morpholinos used are:

fgf8, GAGTCTCATGTTTATAGCCTCAGTA;
nacre, CATGTTCAACTATGTGTTAGCTTCA;
fgf3, CATTGTGGCATGGCGGGATGTCGGC; and
spry4, GGAACCCTTGACTCCATCTGTAGGT.

For both mRNA and morpholino injections, embryos were dechorionated using Pronase and injected with either RNA or morpholinos diluted in 0.2% Phenol Red and 0.1 M KCl, using an Eppendorf 5426 microinjector.

Bead implantations and inhibitor treatment

Bead implantations was performed as described (Reifers et al., 2000). FGF8b- or PBS-soaked control beads were implanted in indicated brain regions of wild-type embryos at the 14 somite stage, the embryos were fixed at 24 hours prior to in situ hybridization. For pharmacological inhibition of FGFR activity, wild-type embryos were treated with 40 mM SU5402 (Calbiochem; Mohammadi et al., 1997) in embryo medium at 28.5°C in the dark.

RESULTS

Isolation of *sprouty4*

To identify genes with restricted expression patterns during zebrafish embryogenesis, we are currently carrying out a large scale in situ hybridization screen. One of the clones isolated by this approach displayed an expression pattern extremely similar to *fgf8* (Fürthauer et al., 1997; Reifers et al., 1998) and *fgf3*. Sequencing of this clone revealed that it contained the partial coding sequence of a zebrafish Sprouty homolog (Hacohen et al., 1998). We obtained a full-length cDNA by screening a blastula/gastrula stage library (a gift from Thierry Lepage).

The zebrafish Spry cDNA codes for a 310 amino acid protein. It is most closely related to mouse Sprouty4, the two proteins displaying 65.7% overall amino acid similarity while showing less than 50% amino acid similarity with the mouse or human Spry1, Spry2 and Spry3 (Minowada et al., 1999). Phylogenetic analysis further confirms that our clone encodes a zebrafish Sprouty4 homolog (Fig. 1). Alignment of the peptide sequence of the sprouty genes reveals the existence of three domains of particularly extensive conservation (Fig. 1). Most prominent among these is the C-terminal 130 amino acid cysteine-rich domain, which constitutes the distinctive feature of Spry proteins and has been shown to be sufficient for the localization of Spry at the plasma membrane (Casci et al., 1999). In zebrafish Spry4 this domain contains 25 cysteine residues, 17 of which are found at conserved positions in all Spry proteins.

In addition, the alignment of the vertebrate family members highlights the existence of two short stretches of similar amino acids corresponding to the positions 37-56 and 106-120 of zebrafish Spry4 (Fig. 1). The second of these stretches is remarkably rich in serine (nine out of 15 residues).

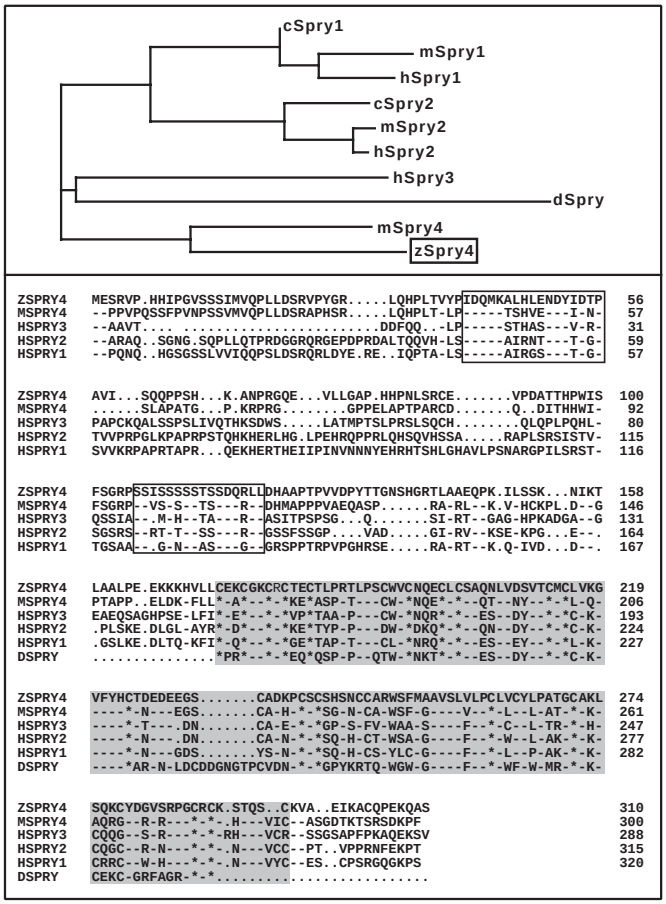


```
ZSPRY4   MESRVP.HHIPGVSSSIMVQPLLDSRVPYGR.....LQHPLTVYPIDQMKALHLENDYIDTP   56
MSPRY4   --PPVPQSSFPVNPSSVMVQPLLDSRAPHSR.....LQHPLT-LP-----TSHVE---I-N-   57
HSPRY3   --AAVT.... .......................DDFQQ..-LP-----STHAS---V-R-   31
HSPRY2   --ARAQ..SGNG.SQPLLQTPRDGGRQRGEPDPRDALTQQVH-LS-----AIRNT---T-G-   59
HSPRY1   --PQNQ..HGSGSSLVVIQQPSLDSRQRLDYE.RE..IQPTA-LS-----AIRGS---T-G-   57

ZSPRY4   AVI...SQQPPSH...K.ANPRGQE...VLLGAP.HHPNLSRCE.......VPDATTHPWIS  100
MSPRY4   ......SLAPATG...P.KRPRG........GPPELAPTPARCD.......Q..DITHHWI-   92
HSPRY3   PAPCKQALSSPSLIVQTHKSDWS.....LATMPTSLPRSLSQCH.......QLQPLPQHL-   80
HSPRY2   TVVPRPGLKPAPRPSTQHKHERLHG.LPEHRQPPRLQHSQVHSSA.....RAPLSRSISTV-  115
HSPRY1   SVVKRPAPRTAPR...QEKHERTHEIIPINVNNNYEHRHTSHLGHAVLPSNARGPILSRST-  116

ZSPRY4   FSGRPSSISSSSSSTSSDQRLLDHAAPTPVVDPYTTGNSHGRTLAAEQPK.ILSSK...NIKT  158
MSPRY4   FSGRP--VS-S--TS---R--DHMAPPPVAEQASP......RA-RL--K.V-HCKPL.D--G  146
HSPRY3   QSSIA--.M-H--TA---R--ASITPSPSG...Q.......SI-RT--GAG-HPKADGA--G  131
HSPRY2   SGSRS--RT-T--SS---R--GSSFSSSGP....VAD.....GI-RV--KSE-KPG...E--.  164
HSPRY1   TGSAA--.G-N--AS---G--GRSPPTRPVPGHRSE.....RA-RT--K.Q-IVD...D--.  167

ZSPRY4   LAALPE.EKKKHVLLCEKCGKCRCTECTLPRTLPSCWVCNQECLCSAQNLVDSVTCMCLVKG  219
MSPRY4   PTAPP..ELDK-FLL*-A*--*-*KE*ASP-T---CW-*NQE*-*--QT--NY--*-*L-Q-  206
HSPRY3   EAEQSAGHPSE-LFI*-E*--*-*VP*TAA-P---CW-*NQR*-*--ES--DY--*-*C-K-  193
HSPRY2   .PLSKE.DLGL-AYR*-D*--*-*KE*TYP-P---DW-*DKQ*-*--QN--DY--*-*C-K-  224
HSPRY1   .GSLKE.DLTQ-KFI*-Q*--*-*GE*TAP-T---CL-*NRQ*-*--ES--EY--*-*L-K-  227
DSPRY    ..............*PR*--*-*EQ*QSP-P--QTW-*NKT*-*--ES--DY--*-*C-K-

ZSPRY4   VFYHCTDEDEEGS.......CADKPCSCSHSNCCARWSFMAAVSLVLPCLVCYLPATGCAKL  274
MSPRY4   ----*-N---EGS.......CA-H-*-*SG-N-CA-WSF-G----V--*-L--L-AT-*-K-  261
HSPRY3   ----*-T----.DN.......CA-E-*-*GP-S-FV-WAA-S----F--*-C--L-TR-*-H-  247
HSPRY2   ----*-N----.DN.......CA-N-*-*SQ-H-CT-WSA-G----F--*-W--L-AK-*-K-  277
HSPRY1   ----*-N---GDS.......YS-N-*-*SQ-H-CS-YLC-G----F--*-L--P-AK-*-K-  282
DSPRY    ----*AR-N-LDCDDGNGTPCVDN-*-*GPYKRTQ-WGW-G----F--*-WF-W-MR-*-K-

ZSPRY4   SQKCYDGVSRPGCRCK.STQS..CKVA..EIKACQPEKQAS                       310
MSPRY4   AQRG--R-R---*-*-.H---VIC--ASGDTKTSRSDKPF                        300
HSPRY3   CQQG--S-R---*-*-RH---VCR--SSGSAPFPKAQEKSV                       288
HSPRY2   CQGC--R-N---*-*-.N---VCC--PT..VPPRNFEKPT                        315
HSPRY1   CRRC--W-H---*-*-.N---VYC--ES..CPSRGQGKPS                        320
DSPRY    CEKC-GRFAGR-*-*.........................
```

Fig. 1. Phylogenetic tree and sequence alignment of Spry proteins. The complete peptide sequences of human (H) Spry1, Spry2 and Spry3, as well as mouse (M) and zebrafish (Z) Spry4 are aligned with the cysteine rich domain of *Drosophila* (D) Spry. The cysteine-rich domain is shaded and two additional short stretches of similar amino acids are boxed. Dashes indicate identical or similar amino acids, dots indicate gap that have been introduced to optimize the alignment. Stars highlight cysteine residues that are conserved among all Spry proteins. The complete protein sequences of human Spry1 and human Spry3 were deduced from genomic sequences (gb/AC026402 and gb/AC025226, respectively). The zSpry4 sequence has been submitted to GenBank Accession Number, AF371368.

While the initial characterization of *Drosophila* Spry suggested a secretion of the protein (Hacohen et al., 1998), subsequent studies favour an intracellular mode of action (Casci et al., 1999). Our analysis of Spry protein sequences using the Wickonsin Package from GCG did not detect any potential signal peptide for secretion in zebrafish Spry4 or in any of the other vertebrate Sprys. In contrast to this, this same program predicted the existence of a signal peptide at the N terminus of *Drosophila* Spry.

Correlation between *spry4*, *fgf8* and *fgf3* expression patterns

Analysis of *spry4* expression revealed a striking correlation with the expression domains of *fgf8* and *fgf3* (Fig. 2). The expression of both *fgf8* and *spry4* begins at sphere stage, shortly after the activation of the zygotic genome. Transcripts first become detectable at the dorsal margin of the blastoderm (Fig. 2A,B), with *spry4* appearing slightly later and in a larger domain. During late blastula, the expression of *spry4* (Fig. 2D) and *fgf8* extends towards lateral and ventral marginal territories. A similar marginal expression is also observed for *fgf3* (Fig. 2C). During gastrulation, *fgf8* and *spry4* are expressed along a dorsoventral gradient at the margin, the *spry4* expression extending more ventrally than *fgf8* (Fig. 2E,F). After midgastrulation *spry4* starts to be expressed in the primordium of the ventral diencephalon, in which *fgf3* transcripts also accumulate (Fig. 2G,H). At the end of gastrulation *spry4* colocalizes with *fgf8* in the midbrain-hindbrain boundary (MHB) region, but appeared in this domain slightly later than *fgf8* (not shown).

Throughout the segmentation period, *fgf8* and *spry4* are continuously expressed in the telencephalon, a region where *fgf3* is also detectable (Fig. 2I-L). *fgf8* and *spry4* are continuously expressed at the MHB, and display similar transient expressions in the hindbrain (Fig. 2I,J) and in the heart primordia (not shown). Posteriorly, *fgf8* and *spry4* are expressed in the paraxial mesoderm, *fgf8* being expressed in the somites, as well as in the anterior aspect of the unsegmented paraxial mesoderm (Fig. 2M), while *spry4* is restricted to the already formed somites (Fig. 2N).

From 24 to 48 hours of development, *spry4* is coexpressed with *fgf8* in the anterior telencephalon, the epiphysis, the optic stalk and the isthmic region (Fig. 2O,P). In addition, it displays a strong expression in branchial arches similar to *fgf3* (Fig. 2Q,R).

By our detailed analysis it appears that in most cases *spry4*, *fgf8* and *fgf3* expression domains overlap, with the expression of *spry4* being somewhat more widespread. However, in a few instances, *fgf8* and *spry4* are expressed in adjacent or in complementary domains.

In the otic region, *fgf8* is expressed in the posterior vesicular epithelium, while *spry4* is detected in a few cells outside of the vesicle (Fig. 2S,T). Adjacent expressions of *fgf8* and *spry4* are furthermore observed in the hypophysis, as well as the forming pectoral fins. Although *fgf8* is expressed in the adenohypophysis, *spry4* is detected in adjacent neurohypophysal cells (Fig. 2U-V). In the fin buds, *fgf8* transcripts are localized to the apical ectodermal ridge (AER), whereas *spry4* is expressed in the underlying mesenchyme (Fig. 2W,X). A similar situation is observed in the caudal fin (not shown).

spry4 expression is dependent on FGF signaling

The strong correlation observed between the expression territories of *spry4*, *fgf8* and *fgf3* suggests that *spry4* expression may be under the control of the FGF signaling pathway.

To investigate whether *spry4* is an in vivo target of Fgf8, its expression was analysed in the *acerebellar* (*ace*) mutation that inactivates the *fgf8* gene, causing in homozygous embryos loss of MHB and cerebellum (Brand et al., 1996; Reifers et al., 1998). Expression of *spry4* is never activated at the isthmic primordium and the anterior hindbrain in *ace* mutant embryos (Fig. 3A,B). During early somitogenesis, expression in the fore- and hindbrain is strongly reduced, while the MHB expression is absent (Fig. 3C,D). At 30 hours of development, expression of *spry4* at the MHB, the dorsal diencephalon, the nasal and facial ectoderm is absent (Fig. 3E,F). Beside the

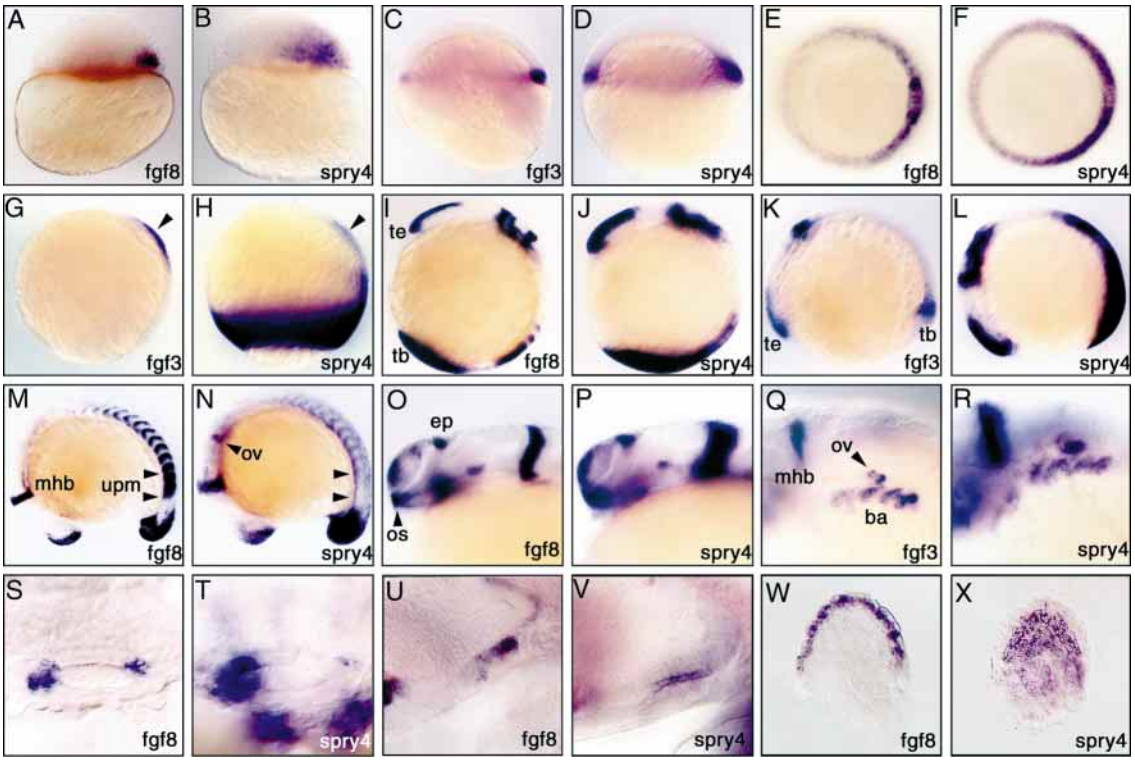

Fig. 2. *fgf8*, *fgf3* and *spry4* are co-expressed during the first 48 hours of embryonic development. (A-H) Blastula and gastrula stages, dorsal towards the right. (A,B) Sphere stage. Expression of *fgf8* and *spry4* at the dorsal margin. (C,D) Expression of *fgf3* and *spry4* in the marginal blastoderm of late blastula stage embryos. (E,F) Vegetal pole view of the dorsoventral expression gradient of *fgf8* and *spry4* at the margin of mid-gastrula stage embryos. (G,H) At late gastrula stages *fgf3* and *spry4* are co-expressed in the ventral forebrain primordium (arrowhead). (I-N) Segmentation stages. Anterior is upwards in (I,J) and towards the left in (K-N). (I-L) Early segmentation stages. *fgf8*, *fgf3* and *spry4* are expressed in the telencephalon (te). (I,J) *fgf8* and *spry4* display similar expressions in the isthmus, the hindbrain, the somites and the tail bud (tb). (K) *fgf3* expression is more restricted in the hindbrain and the tail bud. (M,N) 16-somite stage. Expression of *fgf8* and *spry4* in the telencephalon, the midbrain-hindbrain boundary (mhb), somites and tail bud. *fgf8* but not *spry4* is expressed in the anterior unsegmented paraxial mesoderm (upm). *spry4* but not *fgf8* is expressed in the otic vesicle (ov). (O,P,S,T) 24 hour stage: anterior is towards the left. (O,P) Lateral view. *fgf8* and *spry4* are expressed in the telencephalon, the epiphysis (ep), the optic stalk (os) and the MHB. (S,T) Dorsal view. Both genes are expressed in the anterior otic vesicle. Posteriorly, *fgf8* is detectable in the vesicular epithelium, while *spry4* is expressed in adjacent cells outside of the vesicle. (Q,R) 36 hour stage, lateral view, anterior towards the left. *fgf3* and *spry4* are co-expressed in the branchial arches (ba), the MHB and the otic vesicle. (U-X) 48 hour stage. (U,V) Lateral view, anterior towards the left. *fgf8* is expressed in the adenohypophysis, *spry4* in the adjacent neurohypophysis. (W,X) Dorsal views of dissected pectoral fins. *fgf8* is expressed in the apical ectodermal ridge, *spry4* in the underlying mesenchyme.

expression domains in the neuroectoderm, *spry4* transcript levels are reduced in the somites and the tail bud of mutant embryos at early segmentation stage (not shown).

As *spry4* expression domains correlate with the presence of *fgf3* (Fig. 2) we investigated whether Fgf3 was indeed required for *spry4* expression. As no mutation that inactivates *fgf3* is yet available, we took advantage of a novel technology: gene knock-down by morpholino oligonucleotide microinjection (Nasevicius and Ekker, 2000). Morpholinos are chemically modified antisense oligonucleotides that inhibit the translation of target mRNAs by binding to their 5′ untranslated region and interfering with ribosomal positioning (Summerton, 1999). In order to validate this strategy, we first tested if we could phenocopy the *ace* phenotype. After injection of 0.4 pmol of a morpholino directed against *fgf8* (*@fgf8*), 65% of the embryos displayed a loss of the cerebellum. This defect is extremely similar to the *ace* phenotype (Fig. 4A,B).

To rule out the possibility that this phenotype was generated in a nonspecific manner, we injected a second oligonucleotide directed against the microphtalmia-related gene affected in the zebrafish pigmentation mutant *nacre* (Lister et al., 1999). Injection of 2 pmol of the *nacre* morpholino induced the complete loss of neural crest derived pigmentation in 80% of the embryos (Fig. 4D) and its partial reduction in the remaining 20%. In contrast to this, retinal pigmentation was unaffected, similar to what is observed in genetic *nacre* loss-of-function mutants (Fig. 4D). Injection of 10 pmol of the *nacre* morpholino (25 times the amount used for *fgf8*) produced embryos with minor posterior defects without any alteration of MHB (not shown), demonstrating the specificity of morpholino-induced gene inactivation.

After injection of *fgf3* morpholinos, embryos appeared morphologically normal until early somitogenesis. By 15 hours of development, embryos started however to display a general necrosis that caused their death (not shown). This situation prevented us from analysing the requirement of Fgf3 for *spry4* expression at later stages, notably in the forming branchial arches. We were, however, able to study the effect of impaired Fgf3 signaling on *spry4* expression at gastrula and early somitogenesis.

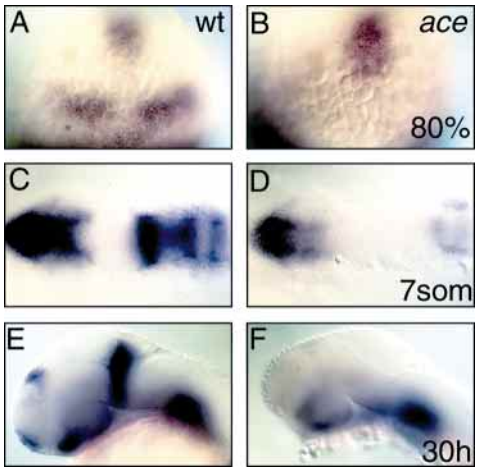

Fig. 3. Expression of *spry4* in wild-type and *acerebellar* (*ace*) embryos. (A,C,E) Wild-type siblings. (B,D,F) Homozygous mutant embryos. (A,B) Dorsal views, anterior towards the top. (C,D) Dorsal views, anterior towards the left. (E,F) Lateral views, anterior towards the left.

At late gastrulation stages, *spry4* and *fgf3*, but not *fgf8*, are co-expressed in the ventral forebrain primordium (Fig. 4E). Microinjection of 0.4 pmol *fgf3* morpholino was found to abolish *spry4* expression in this domain (Fig. 4F). In addition, marginal *spry4* expression appeared slightly reduced. This may be a late consequence of the interference with the earlier action of Fgf3 in the marginal blastoderm.

Loss of Fgf8 function in *ace* mutant leads to the partial reduction of *spry4* expression in the telencephalic region of five somite stage embryos (Fig. 4H). To investigate whether persistent Fgf3 signaling could be responsible for the residual *spry4* expression, we inhibited the function of both Fgf8 and Fgf3 by morpholino injection. Injection of 0.4 pmol *fgf8* morpholino led to a reduction of telencephalic *spry4* expression comparable with that observed in *ace* mutant (Fig. 4H,I). Co-injection of the same amount of *fgf8* morpholino with 0.4 pmol *fgf3* morpholino induced a complete disappearance of *spry4* expression (Fig. 4J). Taken together, our experiments demonstrate that *spry4* expression is also dependent on Fgf3 signaling in several regions of the embryo.

Embryos in which both Fgf8 and Fgf3 function have been inhibited still display residual *spry4* expression in the tail bud (not shown). To further study the requirement of additional FGF signals for the expression of *spry4*, we analysed its expression in embryos where FGF signaling has been blocked pharmacologically. We therefore treated wild-type embryos with SU5402, a potent inhibitor of FGFR1 function (Mohammadi et al., 1997). As SU5402 blocks FGFR1 activity by binding to a region that is conserved in all four FGFRs (Johnson and Williams, 1993), it probably blocks all FGF signals. Wild-type embryos that have been inhibitor treated show a loss of *spry4* expression in all territories at all analyzed stages (from blastula to 24 hours post fertilization(hpf)), as illustrated in Fig. 4K,L. Use of SU5402 therefore demonstrates that other FGFs are responsible for the remaining expression of *spry4* in the tail bud of embryos in which both *fgf8* and *fgf3* have been inhibited by morpholino injection.

Loss-of-function experiments, as well as mutant analysis, therefore showed that Fgf8 and Fgf3 activity are required for *spry4* expression. Using gain-of-function experiments, we further investigated whether Fgf3 and Fgf8 were sufficient to elicit ectopic *spry4* expression.

Microinjection of 25 pg *fgf3* mRNA, into the yolk of two-cell stage embryo results in a massive induction of *spry4* throughout the blastoderm of blastula or gastrula (Fig. 5A,B). Similarly, microinjection of 5 pg *fgf8* mRNA induced the widespread expression of *spry4* throughout the embryo (Fig. 5C). Finally, microinjection of *fgf3* (not shown) or *fgf8* mRNA into a central blastomere at the 16-cell stage (which gives rise to clones located at the animal region of gastrula) resulted in the localized expression of *spry4* at the animal pole, far from its endogenous expression domain (compare Fig. 5D with 5A).

We also locally applied Fgf8-soaked beads during somitogenesis. The implanted Fgf8 bead caused a very strong ectopic induction of *spry4* expression around the bead (Fig.

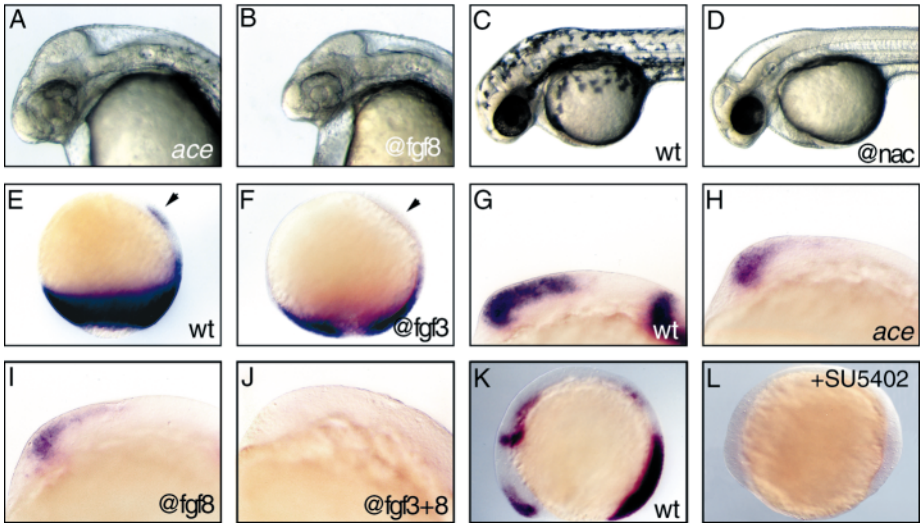

Fig. 4. Inhibition of Fgf3 by antisense morpholino induces loss of spry4 expression. All views are lateral, anterior towards the left, except E,F where anterior is upwards. (A,B) 30 hour stage. Injection of an anti-*fgf8* (@fgf8) morpholino induces a loss of the cerebellum, similar to that observed in *fgf8*/*ace* mutant embryos. (C,D) 36 hour stage. Injection of an anti-*nacre* (@nac) morpholino induces complete loss of neural crest-derived pigmentation. (E,F) Late gastrula stage. Injection of an anti-*fgf3* (@fgf3) morpholino induces a loss of *spry4* expression in the ventral forebrain primordium (arrowhead). (G-J) Telencephalic region of five somite stage embryos. Inactivation of Fgf8 through the *ace* mutation (H) or @fgf8 injection (I) leads to a partial reduction of *spry4* expression. (J) Complete loss of *spry4* transcripts is observed after the simultaneous inhibition of Fgf8 and Fgf3 through co-injection of the corresponding morpholinos. (K,L) Pharmacological inhibition of FGF signaling by treatment with SU5402 leads to complete loss of Spry4. wt, wild type.

5E,F). Taken together these results clearly show that both Fgf3 and Fgf8 are sufficient to induce *spry4* expression.

Misexpression of Spry4 mimics *acerebellar* phenotype

Using gain-of-function experiments, we investigated the effect of Spry4 on embryonic development. Two classes of defects were obtained depending on the amount of *spry4* mRNA injected: an *acerebellar* phenotype at low doses and a ventralization phenotype at higher doses (see below).

At 250 pg *spry4* mRNA, 1% of injected embryos displayed a morphology strikingly similar to the *ace/fgf8* loss-of-function mutant phenotype, which is characterized by a loss of cerebellum (Fig. 6A,B). Moreover, as for *ace* the size of the otic vesicle is reduced. Therefore these observations suggest that Spry4 acts as a Fgf8 antagonist. The low penetrance of the *ace*-like phenotype may reflect the poor stability of the injected RNA, because Fgf8 is required not for the initiation but for the maintenance of the MHB (Reifers et al., 1998). This suggests that an earlier phenotype may exist, but due to the degradation of *spry4* mRNA and persistent fgf8 expression, most of the embryos recovered to wild type. This hypothesis is supported by the analysis of the expression of two early MHB markers, engrailed 2 and pax2.1, known to be the first MHB markers affected in *ace* mutant (Reifers et al., 1998). Expression of these two genes at early somitogenesis in embryos injected with 250 pg of *spry4* mRNA appeared narrower at the MHB for 75% (engrailed 2, 57/76) and 77% (pax2.1, 65/84) (Fig. 6D,F) compared with wild type (Fig. 6C,E). This narrowing of the expression territory at the MHB is identical to that observed in *ace* mutant embryos at early somitogenesis.

As spry4 is the earliest marker known to be expressed at the MHB during gastrulation and because its transcription is under the control of FGF signaling (see Figs 3-5), it was used as a probe to look for an earlier defect in MHB formation. We injected embryos with mRNA comprising only the coding region of *spry4* and then revealed the effect of this injection at late gastrula by in situ hybridization using the 3′UTR of *spry4*. Under these conditions we observed a strong reduction of *spry4* expression (Fig. 6H), reflecting the inhibitory effect of Spry4 on Fgf8 signaling. However, at later segmentation stages, *spry4* expression recovers to wild-type levels (not shown).

In order to improve the penetrance of *ace*-like phenotype induced by *spry4*, we decreased the endogenous Fgf8 dosage. Embryos obtained from crosses between *ace* heterozygous fish and wild type were injected with *spry4* mRNA. Under these conditions, 50% of embryos carried only one copy of *fgf8*. In this sensitized background, loss of cerebellum phenotype, analyzed morphologically at 30 hpf, increased from 1% to 13% (16/123) of the injected embryos. We then tested whether Spry4 could cooperate with an *fgf8* morpholino to induce *ace*-like phenotype. The injection of 0.2 pmol *fgf8* morpholino on its own induces a loss of the cerebellum in only 2% of the embryos. Co-injection of the same amount of *fgf8* morpholino with 250 pg *spry4* mRNA leads to 36% (36/101) of *ace*-like phenotype. Taken together, these results show that Spry4 antagonizes the activity of Fgf8 during MHB formation.

Misexpression of Spry4 ventralizes the embryo

Although low amounts of *spry4* mRNA leads to loss of MHB formation, injection of higher amounts (1 ng) leads to ventralization phenotypes. 42% (70/167) of the embryos showed an expansion of ventral hematopoietic derivatives (Fig. 6J), which is indicative of a weak ventralization. A further 18% (30/167) of injected embryos displayed a reduction of head and notochord as well as a strong increase in hematopoietic derivatives, which are characteristic of a strong ventralization (Fig. 6K,L), or even a complete lack of morphologically recognizable dorsoventral polarity (6%, 10/167, not shown). Finally, 34% (57/167) of injected embryos did not show any dorsoventral patterning defects but displayed various cephalic malformations.

We have previously shown that Fgf8 is involved in the control of the expression of BMPs by inhibiting their expression on the dorsal side of the embryo (Fürthauer et al., 1997). As a consequence, the ventralization phenotype resulting from spry4 overexpression is the expected phenotype for a FGF antagonist. As Fgf8 mediates its effect on the dorsoventral patterning by controlling the BMP expression, we analysed the expression pattern of BMP2b at blastula stage in embryos injected with spry4. For 1 ng of *spry4* mRNA, we observed a strong dorsal expansion of BMP2b expression (Fig. 6N) compared with wild type (Fig. 6M). Similar results were obtained for the expression of BMP4 and BMP7 (not shown). As the result of the extension of BMP expression, genes specifically expressed in presumptive epidermis, such as CG1061, which encodes a forkhead domain-containing protein (M. F., B. T. and C. T., unpublished), appeared to be strongly upregulated (compare Fig. 6P with Fig. 6O, wild type).

Spry4 loss-of-function phenotype

We next investigated the effect of Spry4 loss of function in zebrafish development by inhibiting its expression with morpholino oligonucleotides. Injection of 1 pmol *spry4* morpholino (94%, 51/54) led to embryos with an enlargement of dorsolateral paraxial somitic territories (Fig. 7A,B). This is indicative of a weak dorsalization phenotype consistent with an upregulation of FGF signaling at early developmental stages. This interpretation was further supported by the effect of *spry4* loss of function on BMP2b expression. Upon injection of the same amount of *spry4* morpholino, the expression of BMP2b at the shield stage appeared strongly reduced (but not abolished) in the ventral blastoderm (Fig. 7C,D).

Analysis of various neural markers at early somitogenesis reveals that spry4 loss of function causes a strong enlargement of the telencephalon, visualized by expression of emx1 (Fig. 7E,F). This enlargement of the telencephalic territory may be at the origin of facial outgrowths observed at late developmental stages (Fig. 7G,H). Fgf8 has been shown to direct outgrowth and patterning of the surface ectoderm that overlies the facial primordia in the mouse (Meyers et al., 1998). As a consequence, the phenotype we observed in the zebrafish may result from excessive FGF signaling in the facial mesenchyme.

In conclusion, both our gain- and loss-of-function studies provide evidence that Spry4 affects embryonic development through a modulation of FGF signaling.

Spry4 antagonizes Fgf8 and Fgf3 activity in vivo

We have previously shown that localized misexpression of Fgf8 on the ventral side of the embryo induces the formation

of a partial secondary axis by the local inhibition of BMP gene expression (Fürthauer et al., 1997). Performing the same experiment with Fgf3 gave the same result. To demonstrate the antagonistic effect of Spry4 on Fgf8 and Fgf3, we designed a functional assay in order to inhibit, by overexpression of *spry4*, the formation of a secondary axis resulting from ventral misexpression of Fgf8 or Fgf3 (Fig. 8A).

Two batches of embryos were injected with 200 pg mRNA encoding either β-galactosidase or Spry4. These injections were performed into the yolk of two-cell stage embryos to ensure a widespread RNA distribution. At the 16-cell stage, both sets of embryos were further co-injected into one marginal blastomere with 5 pg *fgf8* (or 25 pg *fgf3*) and 100 pg eGFP mRNA (Fig. 8B). At shield stage, the dorsal side of the embryo was identified by the thickening resulting from the involution of dorsal mesendoderm. We selected the embryos for which the clone of Fgf8- or Fgf3-overexpressing cells lay in the ventral half of the blastoderm (Fig. 8A). When grown at 24 hours, 69.4% of the β-galactosidase/*fgf8*-injected embryos (50/72) displayed either a dorsalized phenotype or the formation of a partial secondary axis (Fig. 8C). In contrast, the frequency of Fgf8-induced phenotypes was reduced to 4.6% (3/65) in *spry4*-injected embryos (Fig. 8C). For *fgf3*, we found that the frequency of Fgf3-induced phenotypes dropped from 58.2% (32/55) to 11.2% (8/71) in presence of Spry4 (Fig. 8D). This establishes clearly that Spry4 is able to antagonize Fgf8 and Fgf3 activity.

Spry4 rescues the dorsalization induced by misexpression of constitutively activated FGFR1

FGFs exert their effects by activating cell-surface receptor tyrosine kinases. Four different FGF receptors have been identified so far and only two of them, *fgfr1* and *fgfr4*, are expressed at early developmental stages in zebrafish (M. F., C. T. and B. T., unpublished). FGFR1 is expressed maternally and its transcripts are widely distributed at blastula stage. During gastrulation, *fgfr1* is expressed in anterior neural plate and in segmental plate mesoderm. At beginning of somitogenesis, *fgfr1* transcripts are observed in the whole head ectoderm with a stronger accumulation at the level of the telencephalon and at the MHB. In MHB, FGFR1 is the only FGF receptor to be expressed (M. F., C. T. and B. T., unpublished). *fgfr4* expression starts at blastula stage in the animal pole region. During gastrulation expression is observed in prechordal plate and in anterior neural plate with a clearing in the expression pattern at the level of the presumptive MHB, as well as at the level of telencephalon and eye field (Thisse et al, 1995). The other two FGF receptors are not expressed before the end of gastrulation. FGFR2 transcripts first appear at early somitogenesis in newly formed somites, while FGFR3 starts to be expressed shortly after gastrulation in presumptive posterior diencephalon and anterior spinal chord (M. F., C. T. and B. T., unpublished). Based on the expression territories of these four FGF receptors, FGFR1 appeared to be the best candidate for the receptor transducing the signal of Fgf8 and Fgf3 at early developmental stages.

To investigate whether Fgf8 and Fgf3 indeed act by stimulating FGFR1, we performed the misexpression of a constitutively activated form of FGFR1 (CA-FGFR1, Umbhauer et al., 2000). This form was generated by fusing a mutated torso extracellular domain with the FGFR1 intracellular domain, thereby inducing a ligand-independent dimerization and activation of the receptor. Injection of 60 pg of CA-FGFR1 mRNA resulted in a strong dorsalization of the embryo (94%, 91/97), a phenotype that was undistinguishable from the dorsalization induced by overexpression of *fgf8* or *fgf3* (Fig. 8E). Conversely, injection of 60 pg of mRNA coding for the CA-FGFR4 (Umbhauer et al., 2000) into embryos at the two-cell stage resulted in various developmental defects unrelated to phenotypes induced upon overexpression of *fgf8* or *fgf3*. This result therefore provides functional evidence that transduction of the Fgf8 and Fgf3 signal is mediated by FGFR1 at early developmental stages.

Spry4 acts downstream of FGFR1

To investigate at which level Spry4 interferes with FGF signaling, we tested its ability to rescue a CA-FGFR1-induced dorsalization. Coinjection of CA-FGFR1 with increasing doses of *spry4* mRNA progressively rescued this dorsalization phenotype. For 125 pg *spry4* mRNA, only 29% (32/109) embryos remain dorsalized while using 250 pg led to a complete rescue of the dorsalization phenotype. This clearly demonstrates that spry4 antagonizes the FGF signaling mediated through FGFR1.

Stimulation of FGFR1 ultimately leads to the phosphorylation of the extracellular-regulated protein kinases (ERK) 1 and 2 (Umbhauer et al., 2000). We therefore took advantage of the use of an antibody recognizing the activated form of ERK (Gabay et al., 1997) to estimate the effect of Spry4 on MAPK activity. In accordance with an activation of ERK after the stimulation of FGFR1, localized misexpression of CA-FGFR1 induces ectopic activation of MAPK at blastula stage (Fig. 8F) whereas activated MAPK is barely detectable in wild-type control embryos (not shown). Conversely, localized injection of 250 pg *spry4* mRNA caused a local inhibition of MAPK activation at mid-gastrula stages (Fig. 8G), when the MAPK is ubiquitously activated in wild-type embryos (not shown).

Our results therefore demonstrate that *spry4* interferes with FGF signaling by acting downstream of FGFR1, leading to a subsequent downregulation of MAPK activity.

DISCUSSION

Relationship between *fgf* and *spry4* expression

The most striking feature of *spry4* expression is its resemblance to that of *fgf8*. We found a closely matching *spry4* expression not only in regions of stable *fgf8* expression (like the telencephalon and the MHB) but also in domains where *fgf8* expression evolves rapidly (like the hindbrain of the early segmentation stage embryo) (Fig. 2). In territories where *spry4* and *fgf8* expression patterns do not correlate, such as ventral diencephalon at late gastrula stage (Fig. 2H) or branchial arches after 24 hours of development (Fig. 2R), we observed a strong correlation between *spry4* and *fgf3* expression patterns. Therefore, *spry4* expression during development is strikingly correlated with the expression sites of *fgf8* and *fgf3*, suggesting that *spry4* may be a target of FGF signaling.

Most frequently, a sharp *fgf* expression domain correlates with a more widespread *spry4* transcription (such as in Fig.

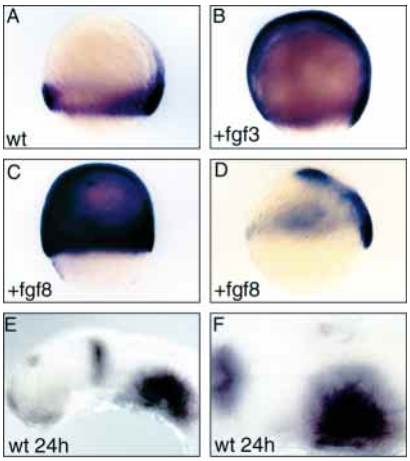

Fig. 5. Fgf8 and Fgf3 induce *spry4*. (A-D) Lateral view of gastrula stage embryos stained for *spry4*. Dorsal is towards the right. (A) Wild type. (B,C) Widespread overexpression of Fgf3 or Fgf8 induces *spry4* throughout the embryo. (D) Microinjection of *fgf8* mRNA in one central blastomere of a 16-cell stage embryo induces *spry4* at the animal pole, far from its endogenous expression domain. (E,F) Implantation of Fgf8-secreting beads induces *spry4* expression. Lateral view (E) and dorsal close-up, anterior towards the left.

2O,P). As Fgf8 is a secreted protein, we suggest that diffusion of growth factors away from the cells that produce it may be at the origin of the expression of *spry4* in cells that lack *fgf8* transcripts. The extent of *spry4* expression may therefore provide a molecular readout of the range of FGF signaling activity during embryonic development. In addition, we have found that following the implantation of Fgf8-secreting beads, the intensity of induced *spry4* expression diminishes as the distance from the bead increases (Fig. 5E,F), suggesting that the induction occurs in a dose-dependent manner. Consistent with this, a dorsoventral expression gradient of *fgf8* at the margin of the gastrula correlates with a similarly graded distribution of *spry4* transcripts (Fig. 2E,F).

In contrast to the usual situation, *spry4* and *fgf8* are expressed in complementary rather than overlapping domains in the hypophysis and the pectoral and caudal fins (Fig. 2U-X). *fgf8* transcripts localize to the adenohypophysis (Fig. 2U), while *spry4* is detected in adjacent neurohypophysal cells (Fig. 2V). An analysis of FGFRs expression in this domain has allowed us to identify the adenohypophysis as a source and the neurohypophysis as a target of FGF signaling: none of the four zebrafish FGFRs is expressed in the adenohypophysis, whereas FGFR2 is detectable in the neurohypophysis (not shown). The lack of a functional FGF signal transduction machinery provides therefore a straightforward explanation for the absence of *spry4* expression in Fgf8-producing adenohypophysal cells. Similarly, the predominant expression of FGFRs in the mesenchymal aspect of the fins suggests that the AER represents a source rather than a target of FGF signaling, explaining thereby its lack of *spry4* expression (Thisse et al., 1995; Poss et al., 2000; M. F., C. T. and B. T., unpublished).

Induction of *spry4* by FGF family members

In *ace* homozygous mutant embryos, *spry4* transcripts are undetectable at the MHB at all developmental stages. As Fgf8 has been shown to be required for the maintenance of this region, it is important to note that *spry4* expression is already abolished at the early developmental stages (Fig. 3) when other

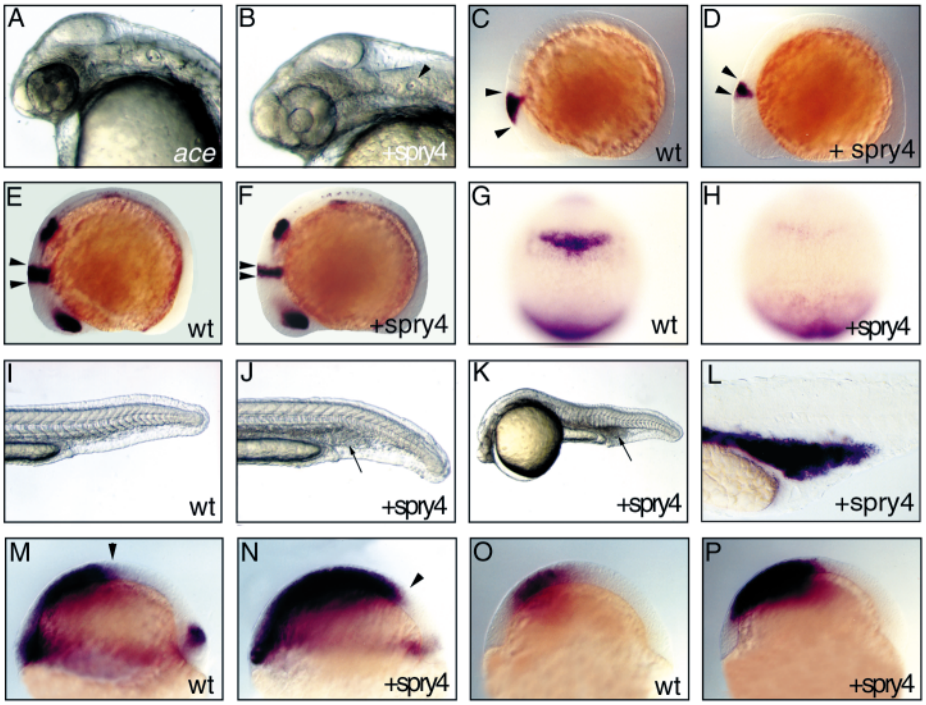

Fig. 6. Effects of gain of Spry4 function on embryonic development. (A,B) Lateral cephalic views of 36 hour embryos. Overexpression of Spry4 by microinjection of 200 pg *spry4* mRNA (B) induces a loss of the cerebellum and reduction of the otic vesicle (arrowhead), similar to the phenotype of *ace* mutant embryos (A). (C-F) Lateral view of 10-somite stage embryos stained for engrailed 2 (C,D) and for pax2.1 in (E,F). (C,E) Wild-type embryo (D,F) and embryo injected with 250pg *spry4* mRNA (D,F). Expression territory of engrailed 2 (D) and pax2.1 (F) (delimited by arrowheads) appears narrower. (G,H) Dorsal view of bud-stage embryos stained for Spry4. Overexpression of Spry4 by microinjection of 200 pg *spry4* mRNA (comprising the ORF only) induces loss of endogenous *spry4* expression at the midbrain-hindbrain boundary (H). (I-L) Injection of 1 ng *spry4* mRNA induces a range of ventralized phenotypes. 30-hour stage, anterior towards the left. Spry4 induces expansion of ventral hematopoietic derivatives (J, arrow compared with wild-type in I), a reduction of cephalic territories and a strong expansion of hematopoietic territory (K) labeled with CB588, a blood-specific marker (L). (M,N) Lateral view of late blastula stage embryo. Expression of BMP2b is expanded dorsally in embryos injected with 200 pg of *spry4* mRNA (N) compared with wild-type (M). Arrowheads delimit the dorsalmost BMP2b expression in ventral non marginal blastomeres. (O,P) Lateral view of a late blastula stage embryo. Expression of an epidermal-specific gene, CG1061, is upregulated in an embryo injected with 200 pg *spry4* mRNA (P). Compare with wild type (O).

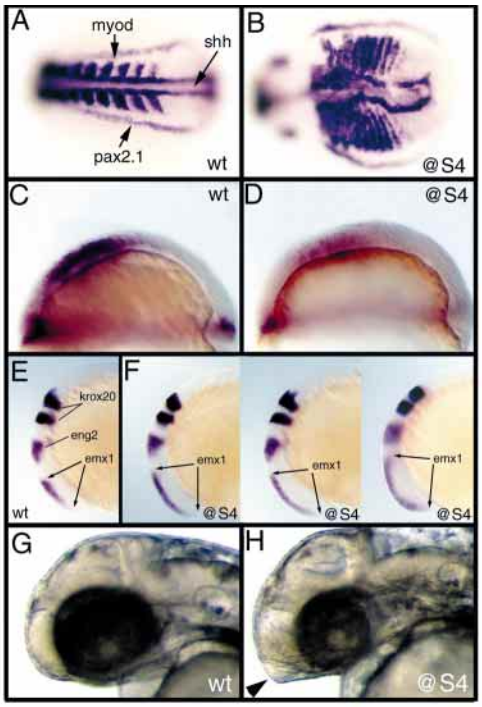

Fig. 7. Effect of loss of Spry4 function on embryonic development. (A,B) Dorsal view of 10-somite stage embryos stained for pax2.1, myod and shh. Inhibition of Spry4 function by injection of *spry4* morpholino (@S4) induces a lateral expansion of the somites (B). (C,D) embryos at late blastula stage on lateral view. Upon injection of @spry4 expression of BMP2b is strongly reduced in ventral blastomeres. (E, F) Lateral view of embryos at the 10-somite stage, labeled for krox20, engrailed 2 (eng2) and emx1. Injection of @spry4 causes a strong enlargement of emx1 expression in telencephalon. (G,H). Lateral cephalic view of 36 hour embryos. Embryos display facial outgrowings (arrowhead) following the injection of @Spry4, probably resulting from early enlargement of telencephalon.

MHB markers, like pax2.1 and engrailed 2 are still expressed (Reifers et al., 1998). The absence of *spry4* expression in this territory is therefore directly related to the impairment of Fgf8 signaling, and not just a secondary consequence of the loss of the isthmic region.

In contrast, a complete loss of *spry4* expression in the telencephalon requires the simultaneous inhibition of both Fgf3 and Fgf8 (Fig. 4I,J). These two growth factors appear to act redundantly in the forebrain, at least as far as the induction of their common target gene *spry4* is concerned.

Loss of Fgf8 function does not affect the expression of *spry4* in the neurohypophysis and the fin bud mesenchyme, suggesting that *spry4* induction there is mediated mainly by other factors. Consistent with this, *spry4*-expressing cells in the neurohypophysis are surrounded not only by *fgf8*-expressing adenohypophysal cells but also by Fgf3-producing cells in the ventral hypothalamus (not shown).

In the mouse embryo, inactivation of Fgf8 has been shown to cause a complete loss of *spry4* expression, suggesting that Fgf8 may be its unique inducer (Minowada et al., 1999). In contrast to this, we have shown that zebrafish *spry4* responds to signaling by several FGF family members.

Drosophila spry has been shown to respond not only to FGF

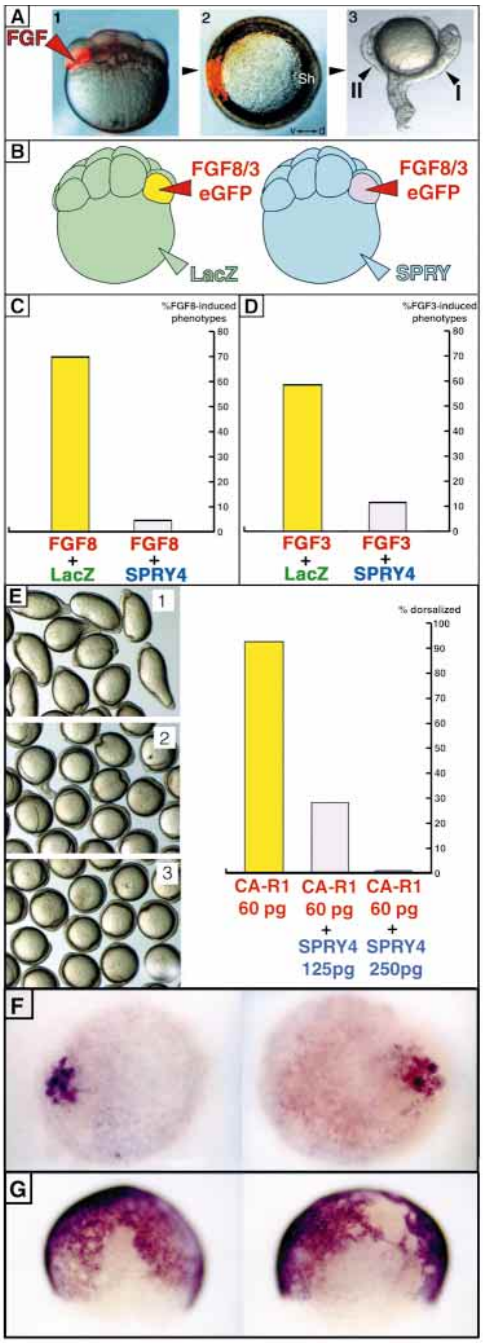

Fig. 8. Spry4 antagonizes FGF signaling pathway in vivo. (A1) *fgf8* (or *fgf3*) mRNA is injected with rhodamine dextran into one blastomere of the 16 cell stage embryo. (A2) If the progeny of the injected cells comes to lie in the ventral aspect of the early gastrula, a secondary embryonic axis is formed (A3). (B) At the 16-cell stage, two batches of embryos that have been previously saturated with *lacZ*- or *spry4*-mRNA are co-injected into one blastomere with eGFP- and *fgf8* (or *fgf3*) mRNA. The GFP allows to identify ventrally located clones. Spry4 inhibits the effect of ventral Fgf8 misexpression (C) or ventral Fgf3 misexpression (D). (E) Injection of 60 pg CA-FGFR1 (CA-R1) strongly dorsalizes embryos (1) co-injection of 125 pg (2) or 250 pg *spry4* mRNA (3) progressively rescues the dorsalized phenotype to wild type. (F) Localized injection of CA-FGFR1 in one blastomere at the 16-cell stage induces a strong activation of ERK at blastula stage. (G) Overexpression of *spry4* inhibits activation of MAPK at gastrula stage.

signaling, but also to activation of the EGF, *torso* and *sevenless* receptor tyrosine kinases (Casci et al., 1999). To investigate whether FGFR-independent pathways are important for *spry4* expression, we have used the pharmacological inhibitor SU5402 (Fig. 4K,L). Nevertheless, in addition to FGF signaling, SU5402 also affects signaling by the vascular endothelial growth factor (Vegf) receptor (Mohammadi et al., 1997). Zebrafish Vegf is, however, unlikely to act as an inducer of *spry4*, as neither Vegf itself nor its receptor (Flk1) display extensive co-expression with *spry4* (Liang et al., 1998; Liao et al., 1997). As FGF inhibitor treatment results in a complete loss of *spry4* expression, this shows that spry4 responds only to FGF signaling.

Antagonistic effect of spry4 on Fgf8 and Fgf3 signaling

The first member of the Sprouty family was initially isolated in *Drosophila* as an antagonist of FGF signaling during tracheal morphogenesis. Correlation between expression patterns of *fgf8, fgf3* and *spry4* suggest that members of Spry family in vertebrate may have a similar FGF antagonistic function. We tested functionally this hypothesis using gain- and loss-of-function experiments. By microinjection of low amount of *spry4* mRNA we were able to generate phenotypes similar to loss of *fgf8* function (as observed in *acerebellar* mutation or after *fgf8* morpholino injection), which are characterized by the lack of cerebellum and the reduction of otic vesicle size (Fig. 6B). Injection of higher amount of *spry4* mRNA gave rise to ventralization phenotype, which reflects alteration of dorsoventral patterning (Fig. 6I-L). This phenotype coincides with the role of Fgf8 at early developmental stages that we previously showed to be dorsal inhibitor of BMP gene expression (Fürthauer et al, 1997). In accordance with this observation, overexpression of Spry4 results in a dorsal expansion of BMP expression patterns (Fig. 6M,N). Nevertheless, while Fgf8 overexpression induces a dorsalisation of the embryo (Fürthauer et al., 1997), the loss of Fgf8 function in *ace* mutant embryos is accompanied only by minor dorsoventral patterning defects (Reifers et al., 1998). *fgf3* is co-expressed with *fgf8* at blastula stages, and its overexpression also induces a similar dorsalization of the embryo (not shown). This suggests that the two factors act redundantly during the early stages of dorsoventral patterning. The ventralized phenotype that results from Spry4 overexpression could therefore be due to the simultaneous inhibition of the dorsalizing activity of both Fgf8 and Fgf3 and possibly also other FGFs expressed at gastrula stage (Draper et al, 1999). This interpretation is further reinforced by our loss-of-function experiments. Indeed, inhibition of spry4 activity through morpholino oligonucleotide injection gives rise to weak dorsalization phenotypes. This can easily be interpreted as a local upregulation of *fgf8* and *fgf3* signaling that results from the decrease of their feedback inhibitor. These two sets of experiments therefore strongly suggest that Spry4 acts as a functional FGF inhibitor during embryonic development. We therefore designed a functional assay to prove the antagonistic effect of Spry4 on Fgf8 and Fgf3. We showed that Spry4 is able to prevent formation of a partial secondary axis mediated by the ventral overexpression of Fgf8 or Fgf3 (Fig. 8). This establishes for the first time in vertebrates that a member of the Spry family acts in vivo as a functional antagonist of FGF signaling.

FGFR1 transduces the Fgf8 and Fgf3 signal

Signaling by Fgf8 and Fgf3 at early developmental stages can be mediated by only two of the four FGF receptors (FGFR1 and FGFR4) because the other begin to be expressed after the end of gastrulation. While in vitro binding assays strongly suggest that Fgf8 has a higher affinity for FGFR4 than for FGFR1 (Ornitz et al, 1996), the similar phenotypes observed after the targeted inactivation of Fgf8 (Sun et al., 1999) or of FGFR1 (Yamaguchi et al., 1994) in the mouse suggest that FGFR1 is more likely to be the receptor that mediates the FGF8 signaling at early developmental stages in vivo.

In this study we have shown that overexpression of constitutively activated forms of FGFR1 and FGFR4 gives rise to different phenotypes. Only CA-FGFR1 induces a strong dorsalization similar to a misexpression of Fgf8 or Fgf3 (Fig. 8E). Therefore, in zebrafish, FGFR1 is likely to be the receptor that mediates the Fgf8 and Fgf3 activity at early developmental stages.

Implication of FGFR1/Ras signaling in dorsoventral patterning

In *Xenopus*, numerous studies have revealed that the FGFR1/Ras/Raf/MEK/MAPK signaling cascade is implicated in the induction of mesoderm in response to FGF signals (Whitman and Melton, 1992; MacNicol et al., 1993; Umbhauer et al., 1995; Umbhauer et al, 2000). Although our results are in perfect agreement with the involvement of FGFR1 in a signaling pathway leading to activation of MAPK, the contribution of this signaling pathway to early embryonic development appears to be different in the two species: in zebrafish, the Fgf8/Fgf3/FGFR1/Ras signaling pathway is not implicated in mesoderm induction, but rather affects the dorsoventral patterning of the embryo through an early inhibition of ventral BMP expression.

Models of growth factor inhibition

Recent years have led to the isolation of a growing number of growth factor inhibitors (Capdevila and Belmonte, 1999). In some instances, signaling molecules and their inhibitors are expressed in complementary domains. For example, the BMP antagonists chordin and noggin 1 are expressed on the dorsal side of the zebrafish embryo and inhibit the activity of ventrally expressed BMPs (Fürthauer et al., 1999; Miller-Bertoglio et al., 1997). The secretion of BMPs and their antagonists from opposite sides of the embryo results in the formation of a gradient of growth factor activity that ultimately establishes the dorsoventral patterning of the embryo.

In contrast to this, *spry4* and *fgf8* are most frequently expressed in overlapping domains. A similar co-expression is observed for the activin/nodal antagonist antivin, and the zebrafish nodal-related genes *cyclops* and *squint* (Thisse et al., 2000). *spry4* and *antivin* are expressed in response to induction by FGF or activin/nodal signaling, respectively, showing that they act as feedback-inhibitors. The co-expression of a growth factor and its antagonist may affect cell communication in two different ways. First, the differential diffusion of a growth factor and its antagonist may be involved in the shaping of a morphogen gradient, a mechanism that has been shown to pattern the anteroposterior axis of the zebrafish embryo by activin/nodal signaling (Thisse et al., 2000). Alternatively, the delayed induction of an inhibitor by its cognate growth factor

may ensure a temporal limitation of growth factor responsiveness of the target cell population. For example, the pseudoreceptor BAMBI blocks signaling through transforming growth factor β receptors, inducing thereby the desensitization of the embryonic cells to BMP/activin signaling (Onichtchouk et al., 1999).

The strikingly dynamic evolution of *spry4* expression in response to Fgf8 and Fgf3 could be important for both a temporal or a spatial limitation of FGF signaling. Future studies will address the relative importance of these two possibilities.

We thank S. Ekker and V. Korzh for sharing data prior publication. The constructs encoding the constitutively activated FGF receptors were kindly provided by J.-F. Riou. We thank V. Heyer and T. Steffan for technical assistance, and O. Nkundwa and A. Karmim for care of fish. M. F. was funded by the Ministère de l'Enseignement Supérieur de la Recherche and the Ligue Nationale Contre le Cancer. F. R. and M. B. are supported by grants from the Deutsche Forschungsgemeinschaft (SFB317) and the Max-Planck-Society (to M. B.). B. T. and C. T. were supported by funds from the Institut National de la Santé et de la Recherche Médicale, the Centre National de la Recherche Scientifique, the Hôpital Universitaire de Strasbourg, the Association pour la Recherche sur le Cancer and the Ligue Nationale Contre le Cancer..

REFERENCES

Amaya, E., Musci, T. J. and Kirschner, M. W. (1991). Expression of a dominant negative mutant of the FGF receptor disrupts mesoderm formation in Xenopus embryos. *Cell* **66**, 257-270.

Brand, M., Heisenberg, C. P., Jiang, Y. J., Beuchle, D., Lun, K., Furutani-Seiki, M., Granato, M., Haffter, P., Hammerschmidt, M., Kane, D. A. et al. (1996). Mutations in zebrafish genes affecting the formation of the boundary between midbrain and hindbrain. *Development* **123**, 179-190.

Capdevila, J., and Belmonte, J. C. (1999). Extracellular modulation of the Hedgehog, Wnt and TGF-beta signalling pathways during embryonic development. *Curr. Opin. Genet. Dev.* **9**, 427-433.

Casci, T., Vinos, J. and Freeman, M. (1999). Sprouty, an intracellular inhibitor of Ras signaling. *Cell* **96**, 655-665.

Chambers, D., Medhurst, A. D., Walsh, F. S., Price, J. and Mason, I. (2000). Differential display of genes expressed at the midbrain – hindbrain junction identifies sprouty2: an FGF8-inducible member of a family of intracellular FGF antagonists. *Mol. Cell. Neurosci.* **15**, 22-35.

Draper B. W., Phillips, J. B., Stock, D. W. and Kimmel, C. B. (1999). FGF signaling and mesodermal patterning in the zebrafish embryo. *Dev. Biol.* **210**,151-180.

Fernig, D. G. and Gallagher, J. T. (1994). Fibroblast growth factors and their receptors: an information network controlling tissue growth, morphogenesis and repair. *Prog. Growth Factor Res.* **5**, 353-377.

Fürthauer, M., Thisse, B. and Thisse, C. (1999). Three different noggin genes antagonize the activity of bone morphogenetic proteins in the zebrafish embryo. *Dev. Biol.* **214**, 181-196.

Fürthauer, M., Thisse, C. and Thisse, B. (1997). A role for FGF-8 in the dorsoventral patterning of the zebrafish gastrula. *Development* **124**, 4253-4264.

Gabey, L., Seger, R. and Shilo, B. Z. (1997). In situ activation pattern of Drosophila FGF receptor pathway during development. *Science* **277**, 1103-1106.

Hacohen, N., Kramer, S., Sutherland, D., Hiromi, Y. and Krasnow, M. A. (1998). sprouty encodes a novel antagonist of FGF signaling that patterns apical branching of the Drosophila airways. *Cell* **92**, 253-263.

Johnson, D. E. and Williams, L. T. (1993). Structural and functional diversity in the FGF receptor multigene family. *Adv. Cancer Res.* **60**, 1-41.

Kiefer, P., Strahle, U. and Dickson, C. (1996). The zebrafish Fgf-3 gene: cDNA sequence, transcript structure and genomic organization. *Gene* **168**, 211-215.

Kishimoto, Y., Lee, K. H., Zon, L., Hammerschmidt, M. and Schulte-Merker, S. (1997). The molecular nature of zebrafish swirl: BMP2 function is essential during early dorsoventral patterning. *Development* **124**, 4457-4466.

Kouhara, H., Hadari, Y. R., Spivak-Kroizman, T., Schilling, J., Bar-Sagi, D., Lax, I. and Schlessinger, J. (1997). A lipid-anchored Grb2-binding protein that links FGF-receptor activation to the Ras/MAPK signaling pathway. *Cell* **89**, 693-702.

Kramer, S., Okabe, M., Hacohen, N., Krasnow, M. A. and Hiromi, Y. (1999). Sprouty: a common antagonist of FGF and EGF signaling pathways in Drosophila. *Development* **126**, 2515-2525.

Lamb, T. M. and Harland, R. M. (1995). Fibroblast growth factor is a direct neural inducer, which combined with noggin generates anterior-posterior neural pattern. *Development* **121**, 3627-3636.

Liang, D., Xu, X., Chin, A. J., Balasubramaniyan, N. V., Teo, M. A., Lam, T. J., Weinberg, E. S. and Ge, R. (1998). Cloning and characterization of vascular endothelial growth factor (VEGF) from zebrafish, Danio rerio. *Biochim. Biophys. Acta* **1397**, 14-20.

Liao, W., Bisgrove, B. W., Sawyer, H., Hug, B., Bell, B., Peters, K., Grunwald, D. J. and Stainier, D. Y. (1997). The zebrafish gene cloche acts upstream of a flk-1 homologue to regulate endothelial cell differentiation. *Development* **124**, 381-389.

Lin, X., Buff, E. M., Perrimon, N. and Michelson, A. M. (1999). Heparan sulfate proteoglycans are essential for FGF receptor signaling during Drosophila embryonic development. *Development* **126**, 3715-3723.

Lister, J. A., Robertson, C. P., Lepage, T., Johnson, S. L. and Raible, D. W. (1999). nacre encodes a zebrafish microphthalmia-related protein that regulates neural-crest-derived pigment cell fate. *Development* **126**, 3757-3767.

Lowenstein, E. J., Daly, R. J., Batzer, A. G., Li, W., Margolis, B., Lammers, R., Ullrich, A., Skolnik, E. Y., Bar-Sagi, D. and Schlessinger, J. (1992). The SH2 and SH3 domain-containing protein GRB2 links receptor tyrosine kinases to ras signaling. *Cell* **70**, 431-442.

MacNicol, A. M., Muslin, A. J. and Williams, L. T. (1993). LT.Raf-1 kinase is essential for early Xenopus development and mediates the induction of mesoderm by FGF. *Cell* **73**, 571-583.

Martin, G. R. (1998). The roles of FGFs in the early development of vertebrate limbs. *Genes Dev.* **12**, 1571-1586.

Metzger, R. J. and Krasnow, M. A. (1999). Genetic control of branching morphogenesis. *Science* **284**, 1635-1639.

Meyers, E. N., Lewandoski, M. and Martin, G. R. (1998). An Fgf8 mutant allelic series generated by Cre- and Flp-mediated recombination. *Nat. Genet.* **18**, 136-141.

Miller-Bertoglio, V. E., Fisher, S., Sanchez, A., Mullins, M. C. and Halpern, M. E. (1997). Differential regulation of chordin expression domains in mutant zebrafish. *Dev. Biol.* **192**, 537-550.

Minowada, G., Jarvis, L. A., Chi, C. L., Neubuser, A., Sun, X., Hacohen, N., Krasnow, M. A. and Martin, G. R. (1999). Vertebrate Sprouty genes are induced by FGF signaling and can cause chondrodysplasia when overexpressed. *Development* **126**, 4465-4475.

Mohammadi, M., McMahon, G., Sun, L., Tang, C., Hirth, P., Yeh, B. K., Hubbard, S. R. and Schlessinger, J. (1997). Structures of the tyrosine kinase domain of fibroblast growth factor receptor in complex with inhibitors. *Science* **276**, 955-960.

Nasevicius, A. and Ekker, S. C. (2000). Effective targeted gene 'knockdown' in zebrafish. *Nat. Genet.* **26**, 216-220.

Onichtchouk, D., Chen, Y. G., Dosch, R., Gawantka, V., Delius, H., Massague, J. and Niehrs, C. (1999). Silencing of TGF-beta signalling by the pseudoreceptor BAMBI. *Nature* **401**, 480-485.

Ornitz, D. M., Xu, J., Colvin, J. S., McEwen, D. G., MacArthur, C. A., Coulier, F., Gao, G. and Goldfarb, M. (1996). Receptor specificity of the fibroblast growth factor family. *J. Biol. Chem.* **271**, 15292-15297.

Partanen, J., Schwartz, L. and Rossant, J. (1998). Opposite phenotypes of hypomorphic and Y766 phosphorylation site mutations reveal a function for Fgfr1 in anteroposterior patterning of mouse embryos. *Genes Dev.* **12**, 2332-2344.

Poss, K. D., Shen, J., Nechiporuk, A., McMahon, G., Thisse, B., Thisse, C. and Keating, M. T. (2000). Roles for fgf signaling during zebrafish fin regeneration. *Dev. Biol.* **222**, 347-358.

Reich, A., Sapir, A. and Shilo, B. (1999). Sprouty is a general inhibitor of receptor tyrosine kinase signaling. *Development* **126**, 4139-4147.

Reifers, F., Bohli, H., Walsh, E. C., Crossley, P. H., Stainier, D. Y. and Brand, M. (1998). Fgf8 is mutated in zebrafish acerebellar (ace) mutants and is required for maintenance of midbrain-hindbrain boundary development and somitogenesis. *Development* **125**, 2381-2395.

Reifers, F., Walsh, E. C., Leger, S., Stainier, D. Y. and Brand, M. (2000).

Induction and differentiation of the zebrafish heart requires fibroblast growth factor 8 (fgf8/acerebellar). *Development* **127**, 225-235.

Sternberg, P. W. and Alberola-Ila, J. (1998). Conspiracy theory: RAS and RAF do not act alone. *Cell* **95**, 447-450.

Summerton, J. (1999). Morpholino antisense oligomers: the case for an RNase H-independent structural type. *Biochim. Biophys. Acta* **1489**, 141-158.

Sun, X., Meyers, E. N., Lewandoski, M. and Martin, G. R. (1999). Targeted disruption of Fgf8 causes failure of cell migration in the gastrulating mouse embryo. *Genes Dev.* **13**, 1834-1846.

Tefft, J. D., Lee, M., Smith, S., Leinwand, M., Zhao, J., Bringas, P., Jr, Crowe, D. L. and Warburton, D. (1999). Conserved function of mSpry-2, a murine homolog of Drosophila sprouty, which negatively modulates respiratory organogenesis. *Curr. Biol.* **9**, 219-222.

Thesleff, I. and Sharpe, P. (1997). Signalling networks regulating dental development. *Mech. Dev.* **67**, 111-123.

Thisse, B., Thisse, C. and Weston, J. A. (1995). Novel FGF receptor (Z-FGFR4) is dynamically expressed in mesoderm and neurectoderm during early zebrafish embryogenesis. *Dev. Dyn.* **203**, 377-391.

Thisse, B., Wright, C. V. and Thisse, C. (2000). Activin- and Nodal-related factors control antero-posterior patterning of the zebrafish embryo. *Nature* **403**, 425-428.

Umbhauer, M., Marshall, C. J., Mason, C. S., Old, R. W. and Smith, J. C. (1995). Protein, nucleotide mesoderm induction in Xenopus caused by activation of MAP kinase. *Nature*. **376**, 58-62.

Umbhauer, M., Penzo-Mendez, A., Clavilier, L., Boucaut, J. and Riou, J. (2000). Signaling specificities of fibroblast growth factor receptors in early Xenopus embryo. *J. Cell Sci*. **113**, 2865-2875.

Whitman, M. and Melton, D. A. (1992).Involvement of p21ras in Xenopus mesoderm induction. *Nature* **357**, 252-254.

Yamaguchi, T. P., Harpal, K., Henkemeyer, M. and Rossant, J. (1994). fgfr-1 is required for embryonic growth and mesodermal patterning during mouse gastrulation. *Genes Dev.* **8**, 3032-3044.